Abrupt millennial variability and interdecadal-interstadial oscillations in a global coupled model: sensitivity to the background climate state

Olivier Arzel · Matthew H. England ·
Alain Colin de Verdière · Thierry Huck

Abstract The origin and bifurcation structure of abrupt millennial-scale climate transitions under steady external solar forcing and in the absence of atmospheric synoptic variability is studied by means of a global coupled model of intermediate complexity. We show that the origin of Dansgaard-Oeschger type oscillations in the model is caused by the weaker northward oceanic heat transport in the Atlantic basin. This is in agreement with previous studies realized with much simpler models, based on highly idealized geometries and simplified physics. The existence of abrupt millennial-scale climate transitions during glacial times can therefore be interpreted as a consequence of the weakening of the negative temperature-advection feedback. This is confirmed through a series of numerical experiments designed to explore the sensitivity of the bifurcation structure of the Atlantic meridional overturning circulation to increased atmospheric CO_2 levels under glacial boundary conditions. Contrasting with the cold, stadial, phases of millennial oscillations, we also show the emergence of strong interdecadal variability in the North Atlantic sector during warm interstadials. The instability driving these interdecadal-interstadial oscillations is shown to be identical to that found in ocean-only models forced by fixed surface buoyancy fluxes, that is, a large-scale baroclinic instability developing in the vicinity of the western boundary current in the North Atlantic. Comparisons with modern observations further suggest a physical mechanism similar to that driving the 30–40 years time scale associated with the Atlantic multidecadal oscillation.

1 Introduction

The physical mechanism underlying abrupt millennial-scale DO events initially observed in $\delta^{18}O$ fluctuations in the Greenland ice cores (e.g., Dansgaard et al. 1993) remains one of the most enigmatic aspect of the puzzle buried within paleo proxy records. These DO events are ubiquitous during the past eight glacial cycles (Loulergue et al. 2008) and are associated with the largest and fastest temperature shifts ever recorded in paleoclimate archives, with Greenland warmings of 8–16°C in annual mean within a few decades (see Wolff et al. 2010, for a review). While it is generally accepted that the Atlantic Meridional Overturning Circulation (AMOC) is somehow involved, a complete and detailed description of the physical mechanism driving this abrupt millennial variability is still lacking and a number of hypotheses have been proposed. Although extremely interesting, it is fair to state that these hypotheses have not led to any deep understanding as to why a millennial oscillation in the Greenland Ice Core records occurs during Marine Isotope Stage 3 (MIS 3, 28-60 thousand of years before present, hereafter ka).

Despite this general agreement, a spectrum of physical mechanisms have been proposed allowing quasi-periodic transitions between different modes of operation of the AMOC, such as stochastic or coherence resonance. The latter concept was used by Timmermann et al. (2003) to

O. Arzel (✉) · M. H. England
Climate Change Research Centre (CCRC),
The University of New South Wales, Sydney, Australia
e-mail: Olivier.Arzel@univ-brest.fr

O. Arzel · A. C. de Verdière · T. Huck
Laboratoire de Physique des Océans (LPO),
Université de Bretagne Occidentale, Brest, France

show that, for realistic freshwater noise levels, abrupt millennial-scale climate transitions can be triggered by an initial meltwater pulse mimicking a Heinrich event, provided that the magnitude of the perturbation is large enough. This process ultimately led the authors to interpret the Bond cycle (Bond et al. 1992) as a coupled ocean-cryosphere oscillation, where the ice-sheet buildup during the successive and relatively long stadials leads, in a 8,000 year period, to initiate a surge once a specified stability threshold is reached. Additional hypotheses based on internal ocean dynamics, under steady external forcing and in the absence of stochastic forcing or geostrophic turbulence in both the atmosphere and the ocean, have also been put forward to explain the emergence of abrupt millennial-scale thermohaline oscillations. These studies first pointed to an increase in polar freshwater forcing (Winton and Sarachik 1993; Sakai and Peltier 1997). The reader is referred to Clement and Peterson (2008), Kageyama et al. (2010) and Arzel et al. (2010) for a more detailed description of existing hypotheses.

Enhanced polar freshwater flux from the atmosphere during the last glacial period is however not supported by analyses of annual layer thicknesses in Greenland ice cores, which appear to be much smaller than Holocene values (Rasmussen et al. 2006; Svensson et al. 2008). This indicates that the freshwater input from the atmosphere at high northern latitudes in the Atlantic basin was weaker than today. As a consequence, the hypothesis that the reduced stability of glacial climates is caused by a stronger hydrological cycle is questionable. Instead, reconstructions of deuterium excess in the Greenland Ice Core Project (GRIP) climate record reveal a large-scale reorganization of the hydrological cycle at both orbital and millennial scales, with a southward shift of the Greenland moisture source during cold periods (Masson-Delmotte et al. 2005).

New possibilities emerged when Winton (1997) showed that millennial oscillations occurred spontaneously in a 2D model when the mean surface air temperature is low enough. The nonlinearity of the seawater equation of state was shown to be the source of the instability: as the climate cools down, polar surface water becomes less able to maintain convection by an upward thermal buoyancy flux and thus is more susceptible to stratification by the downward buoyancy flux associated with surface freshening. Using the same atmospheric heat transport divergence and surface freshwater flux as Winton (1997) and a fully non-linear seawater equation of state implemented in a 2D model, Paul and Schulz (2002) obtained similar deep-decoupling oscillations with millennial periods.

Using a linear seawater equation of state by contrast, Loving and Vallis (2005), using a 3D model, were the first to reproduce abrupt millennial oscillations under cooling climates induced by changes in infrared emissivity. The

same effect was reproduced in a 2D ocean model coupled to sea ice and an energy balance model (EBM) of the atmosphere (Colin de Verdière and te Raa 2010), with the objective to unravel the cause of the instabilities of the cooler climates seen in the model. This was made possible because the economy of the model enabled full bifurcation diagrams to be constructed. The deep water always forms in the vicinity of the sea ice edge and therefore the temperature of the sinking waters does not deviate much from the freezing temperature. On the other hand the sea surface temperature (SST) cools by a few degrees in the tropics. Hence, a reduced stratification occurs in cooler climates. So, even if the strength of the circulation remains the same, the oceanic meridional heat transport is bound to fall. But this heat transport is the major regulator of the circulation: if the circulation weakens, the SST gradient increases to drive the circulation back on track. It is the weakening of this regulator that causes the instability of the circulation to occur for lower freshwater forcing in cooler climates. This sensitivity was tested in a more ambitious 3D planetary geostrophic model coupled to similar atmospheric and sea ice components (with the important addition of wind forcing), and the same conclusions were reached (Arzel et al. 2010). In addition, these 3D simulations revealed the existence of strong interdecadal oscillations of the AMOC during the warm phases (i.e interstadials) of the millennial cycle, while stadials remain more stable with no oscillations at all. The instability driving these interdecadal-interstadial oscillations was shown to be identical to the one emerging in stand-alone ocean models forced by fixed surface buoyancy fluxes. Unfortunately, a precise quantitative estimate of model-data differences is not currently possible due to poor temporal resolution and sparsity of paleo-proxy data.

The objective of the present paper is to climb a step further up in the model hierarchy and test the previous ideas in the context of the more realistic UVic global coupled model in a configuration of prescribed continental ice sheets and atmospheric winds. Fixed winds and filtering of geostrophic turbulence both in the ocean and atmosphere remain however two hypotheses that will need to be relaxed in the future, but the price to pay for carrying out 100 kyr eddy resolving simulations remains too high.

This paper is organized as follows. The coupled ocean-atmosphere-sea ice model and experimental design are presented in Sect. 2. The bifurcation structure of millennial oscillations for each background climate state is analysed in Sect. 3 while Sect. 4 describes a typical millennial cycle, along with the mechanisms responsible for the transitions between the weak and strong phases of the millennial oscillation. In agreement with previous studies based on a variety of idealized climate models (Colin de Verdière and te Raa 2010; Arzel et al. 2010), we show in Sect. 5 that it is

the weaker northward oceanic heat transport in the glacial Atlantic Ocean, compared to warmer climates, which is at the heart of the existence of abrupt millennial-scale climate transitions in the UVic model. The influence of atmospheric CO_2 levels on the domain of existence of millennial oscillations is then investigated in Sect. 6. Again in agreement with previous studies conducted with idealized models, strong interdecadal fluctuations develop during warm interstadials in the UVic model. The physical mechanism underlying these interdecadal-interstadial oscillations is investigated in Sect. 7. The comparison of the structure of perturbations with modern observations further suggests a physical mechanism identical to that driving the 30–40 year time scale associated with the Atlantic Multidecadal Oscillation (AMO, Kerr 2000). The paper finally concludes with a summary and a discussion in Sects. 8 and 9, respectively.

2 Model and experimental design

We use the intermediate complexity coupled model described in detail in Weaver et al. (2001), the version 2.8 of the University of Victoria (UVic) Earth System Climate Model (ESCM). This model comprises an ocean general circulation model [Geophysical Fluid Dynamics Laboratory (GFDL) Modular Ocean Model (MOM) Version 2.2] (Pacanowski 1996) coupled to an energy-moisture balance model for the atmosphere and a dynamic-thermodynamic sea ice model (Bitz et al. 2001) of equal global domain and horizontal resolution of 3.6° longitude by 1.8° latitude. In this coarse resolution model version, the Bering Strait is closed. Land surface and dynamic vegetation models are used. The atmospheric transports of sensible heat and moisture are parameterised on the basis of simple turbulent diffusion with fixed (but not uniform) diffusivity coefficients. The ocean model uses a parameterization of the effects of baroclinic eddies after Gent and McWilliams (1990). The ocean vertical grid spacing increases from 50 m at the surface to 450 m at the bottom (19 levels). There is no flux corrections in the model. Although air-sea heat and freshwater fluxes evolve freely in the model, a non-interactive wind field is employed. The wind stress forcing is instead taken from the National Centers for Environmental Prediction-National Center for Atmospheric Research (NCEP-NCAR) reanalysis fields (Kalnay et al. 1996) and averaged over the period 1958–1997 to form a seasonal cycle from the monthly fields. A virtual salt flux boundary condition is used. This unphysical formulation induces a systematic error in sea surface salinity prediction compared to the more natural freshwater flux boundary condition, especially near river mouths (Griffies et al. 2005). Yin et al. (2010) showed however that the difference between two model versions using virtual and freshwater flux boundary conditions is statistically insignificant in most ocean regions. Oceanic vertical mixing rates increase from 0.3 cm^2 s^{-1} at the surface to 1.3 cm^2 s^{-1} at the bottom, according to the profile proposed by Bryan and Lewis (1979). The energy-conserving thermodynamic sea ice model calculates ice thickness, areal fraction, and ice surface temperature. Ice-sheet topography is prescribed using the ICE-4G reconstructions (Peltier 1994). All the simulations are started from the same initial condition, consisting in a dry isothermal atmosphere and an ocean at rest with observed temperature and salinity fields (Levitus and Boyer 1994; Levitus et al. 1994).

This study aims to examine the mean climate conditions that allow the emergence of abrupt millennial-scale climate changes under steady external (solar) forcing, prescribed ice-sheet topography, a fixed seasonal cycle of surface wind stress, and in the absence of geostrophic turbulence in both the atmosphere and the ocean. A large series of numerical experiments has thus been performed under different background climate conditions. Glacial climates differ only in their (prescribed) atmospheric CO_2 concentration (180, 190, 200, 210 and 220 ppm). Orbital forcing conditions and ice-sheet topography are prescribed to their estimated values at 19 ka. The preindustrial climate experiment has an atmospheric CO_2 concentration of 280 ppm, with orbital forcing conditions and ice-sheet topography fixed at their estimated values at year 1800 AD. Atmospheric CO_2 levels in the glacial experiments plays the same role here as the planetary emissivity in the idealized experiments conducted by Loving and Vallis (2005), Colin de Verdière and te Raa (2010) and Arzel et al. (2010). In summary, among six background climates considered herein, five have a glacial baseline while the remaining one uses preindustrial boundary conditions.

In order to probe the bifurcation structure of the model associated with each background climate, we repeat, for each climate state, several 10,000 year long experiments where permanent freshwater flux anomalies, ranging from −0.3 to 0.1 Sv (1 Sv = 10^6 m^{3}s^{-1}), are added to the calculated freshwater flux between 20°N and 50°N in the Atlantic Ocean. These anomalies are compensated uniformly in the other parts of the domain to ensure salt conservation.

3 The bifurcation structure of millennial oscillations

Previous studies realized with idealized climate models have revealed that the nature of the bifurcation diagrams of the AMOC under glacial climate conditions markedly differs from that obtained under modern conditions (Colin de Verdière and te Raa 2010; Arzel et al. 2010). These

studies showed that a window of millennial oscillations always emerges in glacial cases, while warmer climates (without land ice) remain more stable, with either no oscillations at all or with an oscillation window that is shifted towards stronger freshwater fluxes. The bifurcation diagrams obtained with the present global model are in agreement with those results (Fig. 1). Increasing the atmospheric CO_2 levels in the glacial experiments yields a shift of the oscillation window towards stronger (less negative) freshwater fluxes. The origin of this sensitivity will be examined in Sect. 6. For both the warmest glacial climate ($CO_2 = 220$ ppm) and the preindustrial case however, the oscillations disappear to simply leave the remaining thermal and haline Stommel fixed points. An interesting difference from the bifurcation diagrams obtained previously with idealized single-basin models (Colin de Verdière and te Raa 2010; Arzel et al. 2010) is that the exit of the oscillation window in the present case brings the circulation back to the stable thermal fixed point instead of the stable haline fixed point. In other words, the bifurcation sequence described here (stable thermal state–oscillations–stable thermal state–stable haline state) markedly differs from that obtained previously with idealized single-basin models (stable thermal state–oscillations–stable haline state). Note that haline states can be considered as practically stable given the long duration of experiments (i.e 10,000 years).

It is instructive to note that the permanent freshwater flux anomalies for which millennial oscillations occur in the UVic model are always negative (Fig. 1a–d). This shows that the simulated hydrological cycle (with zero anomalous freshwater forcing) is too strong to allow the emergence of such oscillations. Under glacial boundary conditions, it is expected that a more realistic climate model, including a dynamical atmospheric component, will exhibit a significantly weaker northward transport of water vapor than the UVic model does. For instance, Eisenman et al. (2009) showed, on the basis of simulations performed with a coupled general circulation model, that this transport is significantly reduced in response to increased ice-sheet size, consistent with the equatorward displacement of atmospheric stationary waves induced by the interactions with the ice-sheet (Roe and Lindzen 2001). More realistic climate models might therefore be closer to the instability threshold leading to millennial oscillations than the UVic energy-balance model using prescribed winds.

4 Description of the millennial cycle

This section describes a typical oscillation cycle, obtained with the glacial climate using an atmospheric CO_2 concentration of 190 ppm and an anomalous freshwater flux of -0.21 Sv (see Fig. 1b). Timeseries presented in Fig. 2

Fig. 1 Bifurcation diagrams of the AMOC under glacial climate conditions for atmospheric CO_2 concentrations varying from 180 to 220 ppm (**a**–**e**) and under preindustrial climate conditions (**f**). Stable (unstable) states are denoted by *circles* (*crosses*). The *dashed lines* delineate the range of freshwater fluxes for which abrupt millennial-scale transitions occur between the two unstable states. Negative (positive) freshwater fluxes indicate reduced (enhanced) net precipitation
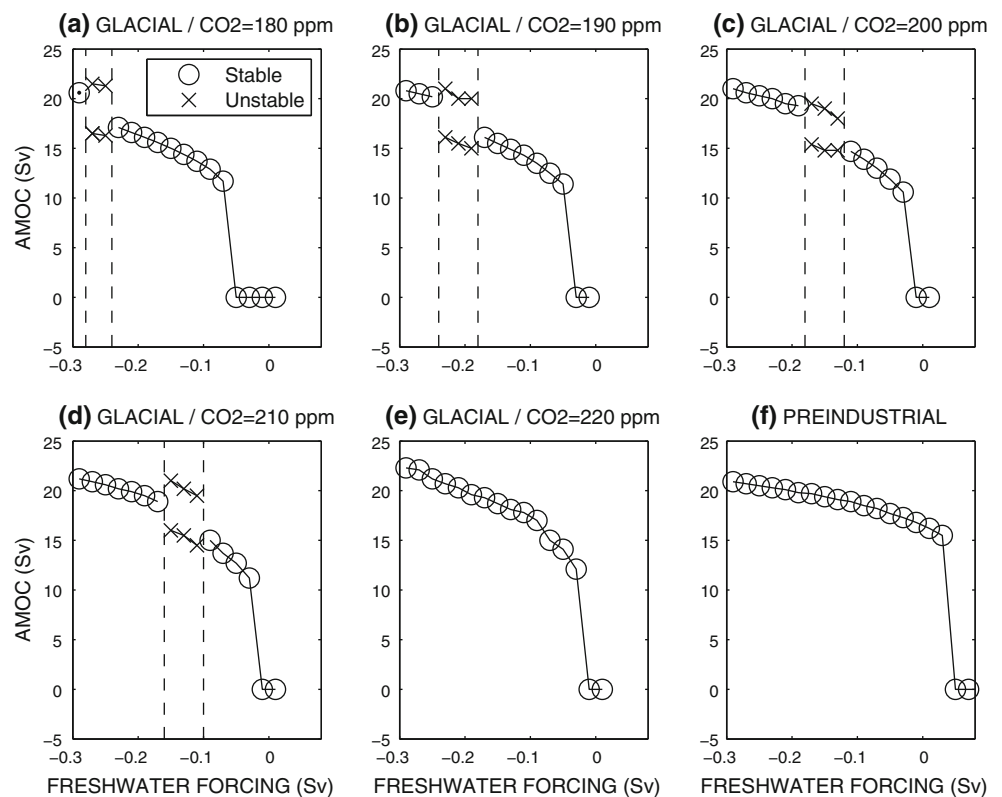
Fig. 2 Timeseries of various physical quantities for the glacial climate using an atmospheric CO_2 concentration of 190 ppm and an anomalous freshwater forcing of −0.21 Sv. The *dashed lines* represent the corresponding values at the nearby stable state, obtained with an anomalous freshwater flux of −0.23 Sv. **a** High latitude (57.6–0°W × 54–70°N) surface air temperature (*SAT*), **b** high latitude (57.6–0°W × 54–70°N) sea surface salinity (*SSS*), **c** global mean ocean temperature, **d** northward oceanic heat transport in the Atlantic basin (1 PW = 10^{15}W), **e** maximum strength of the Atlantic Meridional Overturning Circulation (*AMOC*), **f** globally averaged net radiative forcing at the top of the atmosphere (*TOA*)
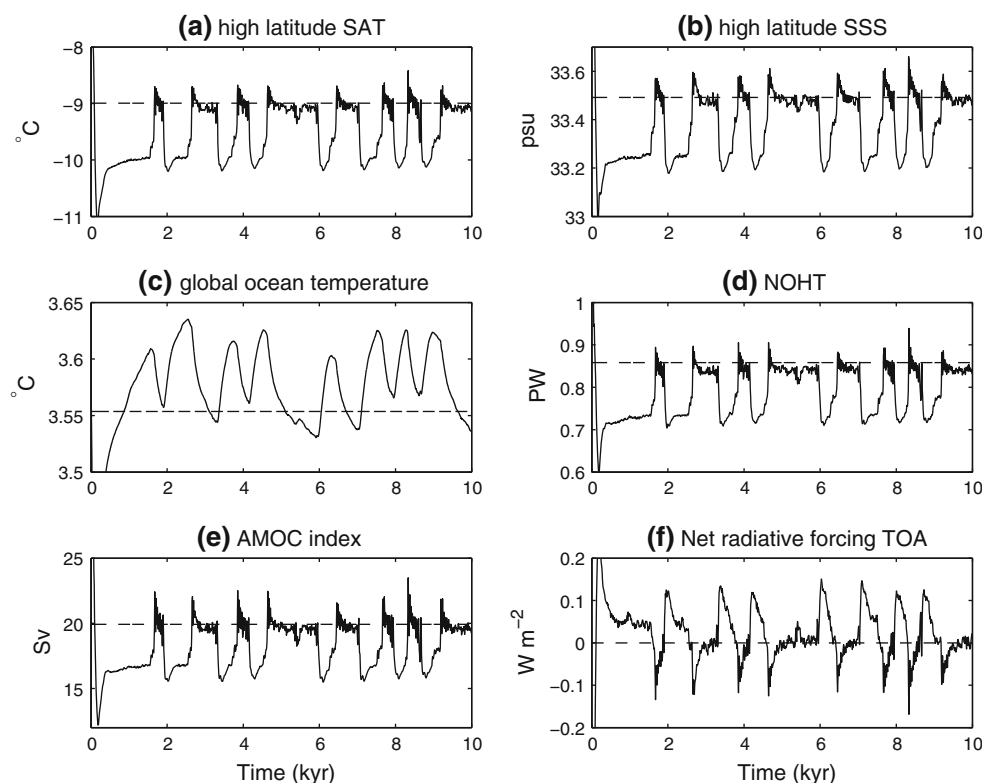
show the emergence of spontaneous abrupt millennial events, with a periodicity varying from 800 to 1,200 years. It is worth noting that the aperiodic character of these millennial oscillations has been obtained without the addition of stochastic noise by contrast to Timmermann et al. (2003). Nonlinear dynamics itself is sufficient to generate nonperiodic oscillations. In agreement with observations, the UVic model reproduces the famous sawtooth shape temperature profile characteristic of DO cycles. There is an abrupt warming operating over a decade or so, followed by a slow cooling phase lasting several centuries, and a rapid decline back to stadial conditions. However, in contrast to the idealized studies of Colin de Verdière and te Raa (2010) and Arzel et al. (2010), the oscillation amplitude in the present case remains relatively weak, with maximum warming peaking at only 1–2°C in the vicinity of the Greenland ice sheet (Fig. 3). The weakness of the oscillation amplitude originates probably from the fact that NADW formation experiences very little spatial variations between the weak and strong phases of the millennial oscillation. This could either be due to the absence of changes in atmospheric circulation in the UVic model or to a strong topographic control of deep convection. Deep water formation occurs only southeast of Iceland in the model, under both glacial and preindustrial climate conditions (Fig. 4). The small meridional displacements of deep convection between the strong and weak phases of the millennial cycle is consistent with the
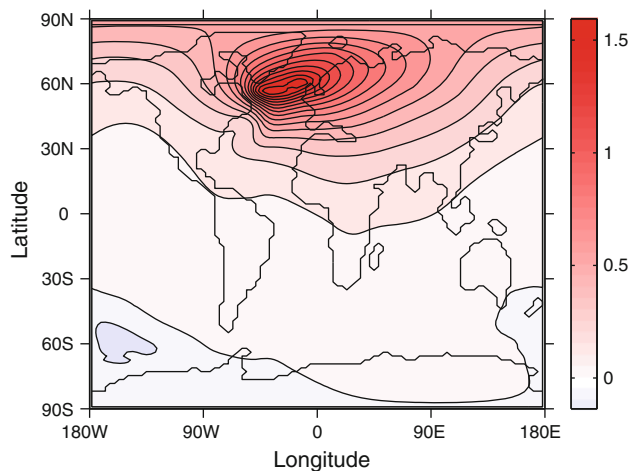
Fig. 3 Typical change in surface air temperature (°C) during stadial-interstadial transitions of the glacial climate using an atmospheric CO_2 concentration of 190 ppm and an anomalous freshwater forcing of −0.21 Sv

relatively small sea ice extent fluctuations, and weak high northern latitude SAT changes. Reconstructions of organic material inputs from terrestrial sources into the subtropical western North Atlantic Ocean reveal that major reorganizations of the atmospheric circulation took place in the North Atlantic sector during stadial-interstadial transitions, with stronger westerlies in the subtropical North Atlantic during Greenland stadials (Lopez-Martinez et al. 2006).

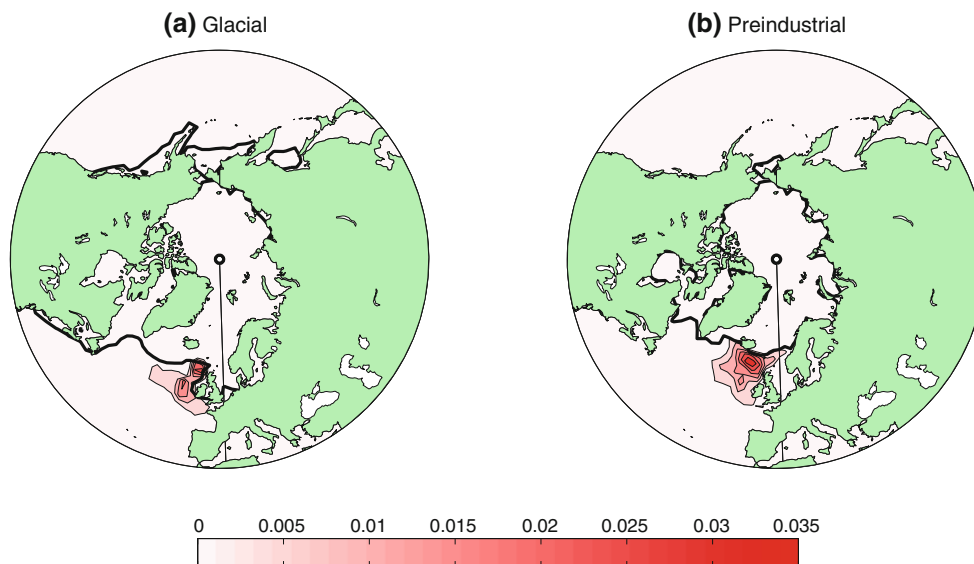**(a)** Glacial   **(b)** Preindustrial

Fig. 4 Sea ice edge location (defined as the 15% sea ice concentration, *thick black line*) and potential energy loss due to convection (*red contours*, W m^{-2}) averaged over the last 1,000 years of each experiment under **a** glacial ($CO_2 = 190$ ppm) and **b** preindustrial conditions for a freshwater forcing $F = -0.29$ Sv. Sea ice cover is overestimated in the Nordic Seas under preindustrial climate conditions, and probably also under glacial climate conditions when compared to the Multiproxy Approach for the Reconstruction of the Glacial Ocean (*MARGO*) (Kucera et al. 2005)

These wind fluctuations have the potential to amplify the atmospheric response to changes in ocean circulation by altering sea ice export and extent. Using an idealized climate model, Colin de Verdière and te Raa (2010) showed that sea ice variations significantly amplify the atmospheric response to changes in ocean circulation. Similarly, using an Atmosphere General Circulation Model (AGCM) forced by sea ice conditions thought to be representative of stadial-interstadial transitions, Li et al. (2010) showed that a significant part of the abrupt warming events surrounding the Greenland ice sheet during the last ice age could originate from large sea ice variations in the Nordic seas. Other factors not represented in the UVic model might also provide a positive feedback on climate, such as those associated with atmospheric methane concentrations which are known, from ice-core records, to have significantly varied in time with DO events (Wolff et al. 2010). The absence of a strong atmospheric signal during stadial-interstadial transitions in the UVic model is consistent with those model results and observations. What needs to be emphasized here is that the shape of the millennial cycle is comparable to that observed, despite the weak amplitude of surface air temperature (SAT) changes. This indicates that the UVic model is at least able to capture some aspects of the mechanisms driving the evolution of temperature changes, as recorded in Greenland ice cores. Finally, since the seasonal cycle of the surface wind-stress forcing is prescribed in our simulations, this suggests that reorganizations of the atmospheric circulation are not essential to the *existence* of abrupt millennial-scale climate transitions.

This contrasts with the hypothesis put forward by Wunsch (2006) who suggested that DO events are a consequence of shifts in the phase of atmospheric stationary waves owing to unstable interactions between the windfield and the continental ice-sheets. This also contrasts from the last two abrupt warmings at the onset of our present warm interglacial period, which were suggested to be triggered by a complete and rapid (one to three years) reorganization of the mid- to high-latitude atmospheric circulation, as deduced from analyses of Greenland dust deposition (Steffensen et al. 2008).

Last, but not least, for each of the quantities presented in Fig. 2, the plateau phase during interstadials coincides with the values of the nearby stable state (dashed lines), in agreement with results obtained using box (Colin de Verdière 2007) and idealized climate models (Arzel et al. 2010). These similarities strongly support the idea that the slower evolution of the coupled system during interstadials owes its existence to the influence of the "ghost" of the nearby saddle-node. The reader is referred to Colin de Verdière (2007) for further details.

Below we describe a typical oscillation cycle and investigate the physical mechanisms that drive the abrupt transitions between the weak and strong phases of the millennial oscillation. As a baseline for our analysis, we focus on the evolution of the coupled system over years 1600–2800 (Fig. 5), a period that includes both an interstadial (years 1650–1950) and a stadial state (years 2050–2550), as well as the corresponding transitions between them.
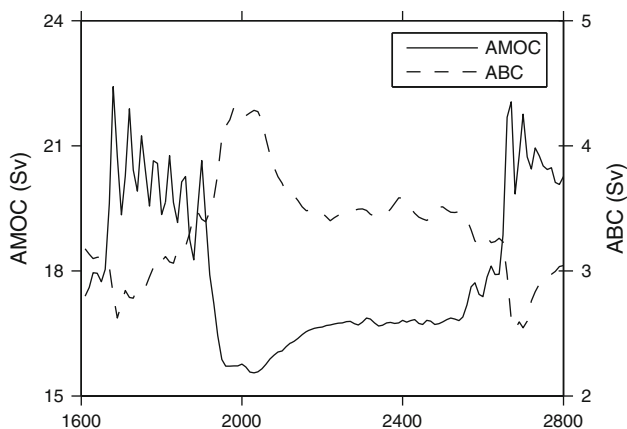
Fig. 5 Same as Fig. 2. Expanded timeseries of the maximum strength of the AMOC (Sv) and of the Atlantic Bottom Cell (*ABC*, anticlockwise) over an oscillation cycle of the glacial climate using an atmospheric CO_2 concentration of 190 ppm and an anomalous freshwater forcing of -0.21 Sv

4.1 Stadial state

Let us first suppose that the system is in its cold state of weak circulation (years 2050–2550). During that period, the AMOC slowly strengthens while the intrusion of Antarctic Bottom Water in the North Atlantic slowly weakens (Fig. 5).

4.1.1 Temperature changes

Figure 6b shows that the vertical structure of temperature changes in the extratropical North Atlantic and Nordic Seas is very similar. There is a gradual warming at the surface and at intermediate depths and a cooling at greater depths. This pattern of temperature changes during stadials agrees reasonably well with paleoceanographic proxy reconstructions (Rasmussen and Thomsen 2004) although the mechanisms through which this pattern is established may differ from what has been inferred from observations.

The heat budget of the extratropical North Atlantic (mid-latitude box in Fig. 6a) shows that the temperature increase experienced by the ocean in the 1240–2990 m depth range during stadials is caused by downward advection of warm surface waters (Fig. 7a, b). This contrasts with a multi-proxy analysis performed by Rasmussen and Thomsen (2004) who suggested that this gradual warming, reminiscent of DO stadials, is caused by northward flowing warm waters associated with the North Atlantic Drift. This also contrasts with previous studies using idealized 2D and 3D models where the temperature increase at intermediate depths was caused by either horizontal mixing with waters from lower latitudes (Colin de Verdière and te Raa 2010) or northward advection of warm tropical waters (Arzel et al. 2010). The present model-data discrepency is likely due to the absence of sea ice at these latitudes during stadials in the model. The presence of sea ice would shift the surface convergence and subsequent downwelling further south, at proximity of the sea ice edge, thereby reducing the influence of vertical motions on extratropical temperature changes below the thermocline.

In the abyssal extratropical North Atlantic, the heat budget analysis reveals that the cooling trend is caused by upward advection which more than compensates for the warming associated with vertical diffusive processes and meridional advection (Fig. 7c, d).
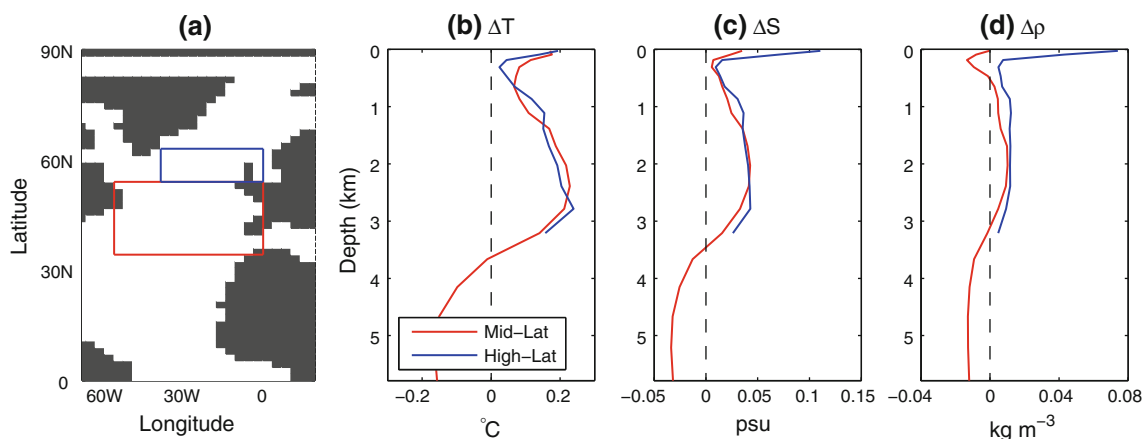

Fig. 6 Horizontally averaged temperature (ΔT), salinity (ΔS) and density ($\Delta \rho$) changes as a function of depth between years 2050–2550 (stadial phase, see Fig. 5) in the two regions shown in the *left panel*, i.e mid-latitude box (57.6–0°W × 34.2–54°N) and high-latitude box (39.6–0°W × 54–63°N), for the glacial climate using an atmospheric CO_2 concentration of 190 ppm and an anomalous freshwater forcing of -0.21 Sv. Changes are calculated from the linear trend over the period. *Red* (*blue*) *solid lines* correspond to the mid-latitude (high-latitude) *box*

Fig. 7 Stadial (years 2050–2550) heat balance of the extratropical North Atlantic Ocean (mid-latitude box in Fig. 6a) in the 1240–2990 m depth range (**a, b**) and for depths greater than 3900 m (**c, d**) for the glacial climate using an atmospheric CO_2 concentration of 190 ppm and an anomalous freshwater forcing of −0.21 Sv. All terms (trend, advection, diffusion, convection) of the heat conservation equation are shown in the *upper panels*. The temperature advection term is splitted into its three components (mutiplied by −1) in the *lower panels*
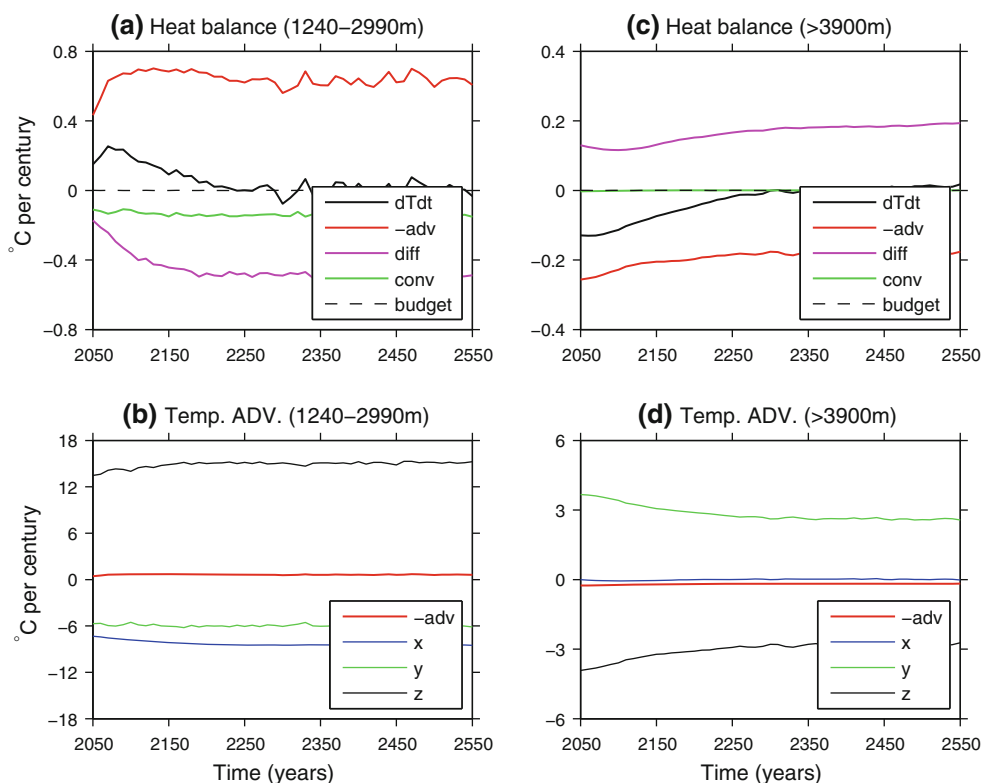
4.1.2 Salinity changes

The pattern of salinity changes is very similar to that of temperature changes from mid-to-high latitudes (Fig. 6c). Corresponding salt budget analyses (not shown) show that the physical processes responsible for the gradual salinity increase at intermediate depths from mid-to-high latitudes and the deep to abyssal mid-latitude freshening are identical to those driving the temperature changes. At the surface however, an increase in sea surface salinity (SSS) during stadials is much larger in the Nordic Seas than at mid-latitudes. The salt budget analysis applied to the surface in the Nordic Seas (Fig. 8) indicates that northward advection of relatively salty waters into the region combined with convective and vertical mixing processes is responsible for the SSS increase there during stadials.

4.2 Stadial-interstadial transition

Can these temperature and salinity changes account for the rapid transition toward the interstadial state? Looking at the pattern of density changes in the extratropical North Atlantic (Fig. 6d), we see that density changes are dominated by temperature changes near the surface, while salinity changes dominate at depth. The stability of the stratification in the extratropical ocean therefore continuously increases during the whole stadial phase. In the Nordic Seas however, a very different picture emerges. This

is due to the relatively strong increase in SSS there (Fig. 6c). This results in a gradual increase in sea surface density that is not present at mid-latitudes. It follows that at some point the water column there becomes unstable. The transition to the interstadial state is then initiated along with the release of heat accumulated at depths for centuries. Therefore, the mechanism of stadial-interstadial transitions in the UVic model strongly contrasts with the extratropical gradual warming at intermediate depths found in deep-decoupling oscillations (Winton and Sarachik 1993). This difference does not imply however that the present simulated variability differs from deep-decoupling oscillations. Our oscillations are indeed characterized by a deep-coupled phase where the circulation is strong and a deep-decoupled phase where the circulation is weak and heat is accumulated in the deep ocean. The only difference between our study and the previous ones resides in the mechanism responsible for the breaking of the polar halocline.

4.3 Interstadial state and return to stadial conditions

The strengthening of the AMOC during stadial-interstadial transitions, referred to as a flush event (Winton and Sarachik 1993), results in increased Arctic sea ice melting and northward oceanic heat transport. These processes tend to decrease the large-scale meridional pressure gradient that partly drives the circulation. As a result, the circulation weakens and the positive salt-advection feedback then
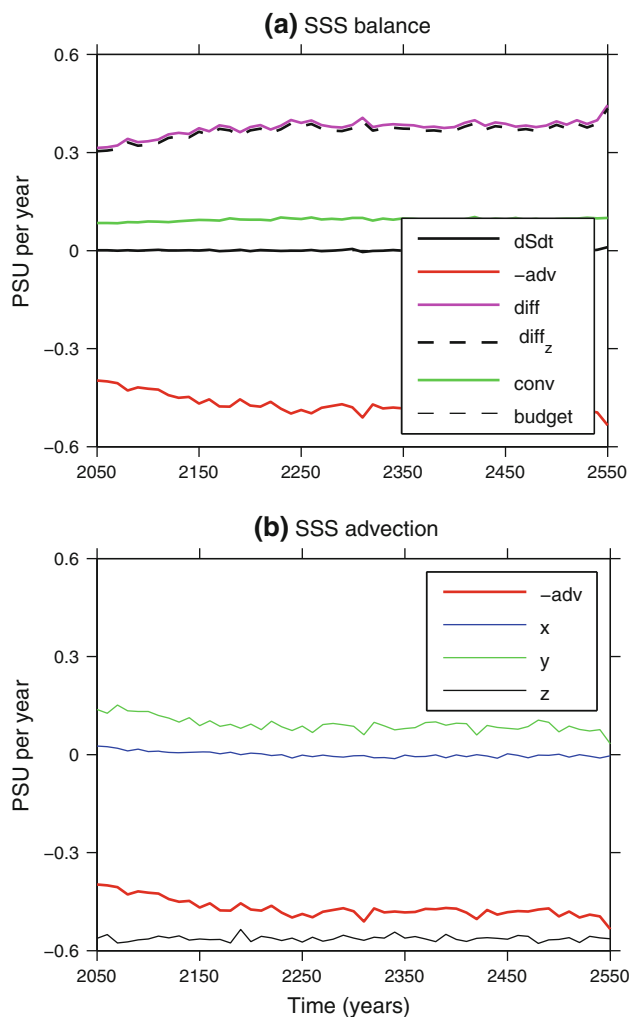
Fig. 8 Stadial (years 2050–2550) SSS balance in the Nordic Seas (high-latitude box in Fig. 6a) for the glacial climate using an atmospheric CO_2 concentration of 190 ppm and an anomalous freshwater forcing of -0.21 Sv. All terms (trend, advection, diffusion, convection) are shown in the *upper panel*. Changes in SSS due to vertical mixing and surface fluxes (diff$_z$) are also shown. The salinity advection term is splitted into its three components (mutiplied by -1) in the *lower panel*

works in reverse and leads to a further weakening of the circulation. When the circulation approaches the nearby saddle node its time evolution slows down. At the same time, a polar halocline slowly forms at high northern latitudes until deep convection cannot be sustained anymore. At this stage, the coupled system is brought back rapidly towards the cold state of weak circulation after which time a new stadial phase starts again.

5 The origin of the reduced stability of glacial climates

In order to understand the origin of the reduced stability of glacial climates, a comparison between the mean climate

states at marginal stability of the coldest glacial climate must be conducted. The comparison is therefore made for an anomalous freshwater forcing F of -0.29 Sv, that is, just prior to the entry into the oscillatory regime of the glacial climate using the lowest atmospheric CO_2 concentration (i.e, 180 ppm). In agreement with the fact that the same anomalous freshwater forcing has been used in these simulations, the oceanic freshwater transport remains almost identical (not shown). The origin of the reduced stability of glacial climates cannot therefore be ascribed to modifications of the oceanic freshwater transport. Figure 9 shows the northward oceanic heat transport in the Atlantic basin across the six background climate states for this particular value of F. In agreement with previous studies conducted with idealized models, glacial climates are clearly less efficient at transporting warm tropical waters poleward. However, the oceanic heat transport associated with the glacial climate using the highest atmospheric CO_2 concentration is similar to that obtained for preindustrial climate conditions, and peaks at a value about 10% stronger than that corresponding to colder climates. The right-top panel in Fig. 9 highlights the significant shift experienced by the glacial oceanic heat transport when the atmospheric CO_2 concentration is increased from 210 to 220 ppm. Interestingly and as noted in a previous section, these two climates, characterized by higher oceanic heat transports, do not exhibit millennial oscillations across their whole bifurcation diagram (Fig. 1). This supports previous hypotheses deduced from idealized model studies (Colin de Verdière and te Raa 2010; Arzel et al. 2010) that the reduced stability of cold climates, that is, the emergence of abrupt millennial-scale climate transitions, is a consequence of their weaker oceanic heat transports compared to warmer climates. As the background climate cools down, the oceanic heat transport decreases, which induces a weakening of the negative temperature advection feedback. At some point, this negative feedback cannot defeat the destabilizing influence that the positive salt-advection feedback exerts on the circulation. This results in an instability of the AMOC, which ultimately sets up an oscillatory regime whose mechanism and characteristics have been presented above.

Crucial to the existence of abrupt millennial-scale climate transitions seems therefore to be the amount of heat carried from low to high latitudes. It is thus natural to investigate the mechanisms that control the sensitivity of this transport to the mean climate state. A close inspection of the shift in oceanic heat transport seen in Fig. 9 reveals that it is caused by an instability of the sea ice edge in response to increasing atmospheric CO_2 levels under glacial boundary conditions. The melt back of sea ice coverage south of Iceland results in an increase of deep convection slightly north of the region where

Fig. 9 a Northward oceanic heat transport (*NOHT*) in the Atlantic basin across the six background climates for a freshwater forcing anomaly $F = -0.29$ Sv. This particular value of F corresponds to that taken at marginal stability of the glacial climate using an atmospheric CO_2 concentration of 180 ppm. **b** Maximum northward oceanic heat transport for each climate case showing a significant shift between the two glacial climates using prescribed atmospheric CO_2 levels of 210 and 220 ppm
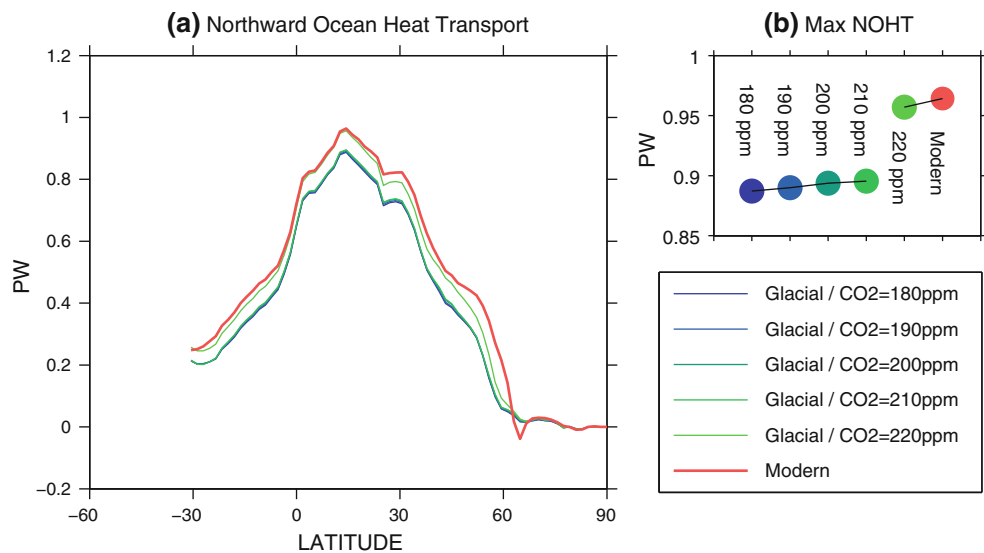
NADW was originally formed under glacial climate conditions using atmospheric CO_2 concentrations of 210 ppm or less. Although deep ocean ventilation remains nearly constant (not shown) in response to this relocation of deep convection, the Atlantic ocean experiences a significant cooling ($\sim 0.5°C$ in the depth range 1–4 km, Fig. 10a). This anomalous cooling is caused by convective motions which bring cold surface waters downwards and warm deep waters upwards. The cold anomaly then spreads across the deep Atlantic basin through diffusive processes and advection by the mean circulation. Such a sensitivity is not seen in any other CO_2 range, and an example is given in Fig. 10b. The corresponding increase in temperature stratification at depths where the AMOC operates implies a substantial increase in northward oceanic heat transport, a change that ultimately tends to stabilize the AMOC associated with the warmest glacial case.

Let us finally mention that, in the UVic model, both the atmospheric circulation (advection terms for temperature and specific humidity) and the atmospheric eddy diffusivity coefficients (for temperature and specific humidity) are prescribed. Hence the atmospheric feedback on the evolution of oceanic perturbations does not change with the mean state of the atmosphere, as easily deduced from a linear stability analysis (see Marotzke 1996). A similar conclusion can be made for the oceanic eddy transports. The influence of the mean climate state on the stability of the coupled system is thus restricted to the oceanic advective terms. Colin de Verdière and te Raa (2010) have indeed shown that the coupling with the atmosphere does not modify the value of the freshwater forcing at the transition from the stable thermal state to the oscillatory regime (see their Fig. 14), confirming that modifications of the atmospheric mean state do not affect the stability of the coupled system.
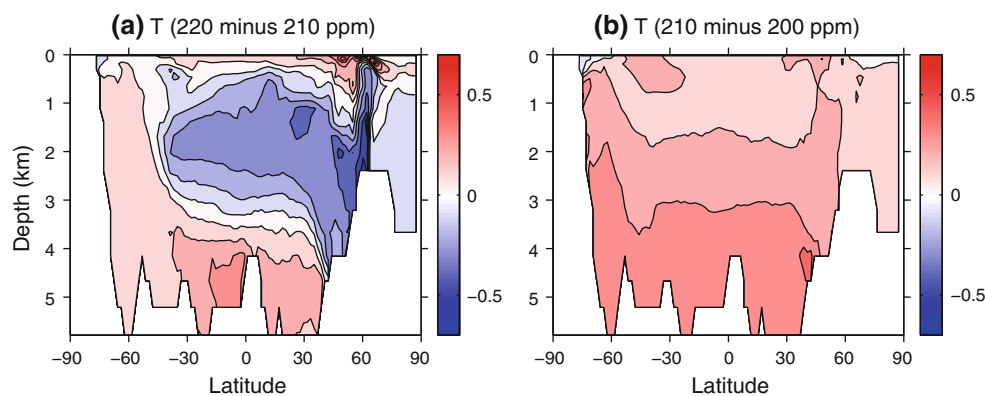

Fig. 10 Zonally-averaged temperature difference (°C) in the Atlantic basin between the glacial climates using atmospheric CO_2 concentrations of **a** 220 and 210 ppm and **b** 210 and 200 ppm for a freshwater forcing $F = -0.29$ Sv, that is, at marginal stability of the coldest glacial climate (i.e, $CO_2 = 180$ ppm). Note the strong increase in temperature stratification when the atmospheric CO_2 concentration is increased from 210 to 220 ppm

6 CO$_2$ influence on the domain of existence of millennial oscillations

The previous section showed that the existence of DO type oscillations in the model is tightly related to the amount of heat carried from low to high latitudes in the North Atlantic Ocean. This however does not give the reason why the oscillation window is shifted toward stronger freshwater fluxes as the atmospheric CO$_2$ concentration is increased from 180 to 210 ppm (Fig. 1) since associated oceanic heat transports are very similar across this range of climates (Fig. 9). The appropriate methodology to infer the origin of this sensitivity is, similar to the previous section, to compare the characteristics of the mean climate states at marginal stability of the coldest glacial climate (i.e, CO$_2$ = 180 ppm), that is, for a freshwater forcing F of -0.29 Sv. The background climates of interest here are glacial climates using atmospheric CO$_2$ levels varying from 180 to 210 ppm. The analysis in what follows is limited to the comparison between the two glacial climates for which the difference in their bifurcation structure is the largest. The comparison is therefore made between the climates using atmospheric CO$_2$ levels of 210 and 180 ppm.

Consistent with the fact that the same freshwater forcing ($F = -0.29$ Sv) has been applied to these two climates, the northward salt transport (at equilibrium) remains almost identical when the atmospheric CO$_2$ concentration is increased from 180 ppm to 210 ppm. Although annual mean sea ice coverage (defined as the area where sea ice concentration exceeds 15%) barely changes in the Nordic Seas between these two climates, both the sea ice concentration and thickness are reduced at proximity of the convection site (-25% and -50 cm, respectively), east of Iceland, under the warm glacial case considered herein. As a consequence, the sea ice to ocean freshwater flux in this area is significantly reduced (-1.4 m year^{-1}). Saltier surface conditions ($+0.5$ psu) therefore result at the convection site under this warm glacial case compared to the coldest one. This implies that stronger freshwater fluxes are required to shut down convection and destabilize the circulation. This is the reason why the oscillation window in Fig. 1 is shifted toward stronger (less negative) freshwater fluxes as the atmospheric CO$_2$ concentration increases from 180 to 210 ppm.

7 Origin of interdecadal-interstadial oscillations

To discuss the origin of interdecadal-interstadial oscillations, we use the same glacial experiment as before (atmospheric CO$_2$ concentration of 190 ppm and a freshwater forcing of -0.21 Sv). As can be seen in Fig. 5, strong interdecadal oscillations of the AMOC tend to occur during warm interstadials, while stadials remain more stable with no oscillations at all. This is in good agreement with results obtained by Arzel et al. (2010) using a single-hemisphere flat-bottom planetary geostrophic ocean model coupled to a dry energy balance model of the atmosphere and a simple thermodynamic sea-ice model. In their simple model, the interdecadal mode of variability was found to be identical to the one emerging in stand-alone ocean models forced by fixed surface (buoyancy) fluxes (see Greatbatch and Zhang 1995; Huck et al. 1999). This internal ocean mode of interdecadal variability was shown to be robust to the coupling with energy balance (Huck et al. 2001) and zonally-averaged statistical-dynamical models of the atmosphere (Arzel et al. 2007) as long as the cumulative damping effect of air-sea turbulent heat fluxes and infrared back radiation is not too strong. While the long-wave limit of the baroclinic instability in the vicinity of the western boundary current was shown to be at the origin of the existence of these interdecadal oscillations (Colin de Verdière and Huck 1999), the strong interplay between the out-of-phase variations of zonal and meridional basin-scale temperature gradients drives the oscillation cycle (te Raa and Dijkstra 2002).

Interestingly, the period of these oscillations ($\sim$35 years) is close to that inferred from bathythermograph measurements and tide gauge records in the North Atlantic (Frankcombe et al. 2008; Frankcombe and Dijkstra 2009). However, the model does not exhibit the longer time scales of 50–70 years also present in the instrumental record (Rayner et al. 2003) and proxy climate archives (Mann et al. 1998). The mechanism associated with this longer time scale is not clear, but it was suggested that it is caused by a different mode of variability involving Arctic-Atlantic exchanges (Frankcombe et al. 2010).

The objective of this section is thus to determine the origin of those interdecadal-interstadial oscillations in the present global coupled model, and then to compare our conclusions with those obtained earlier by Arzel et al. (2010). To do this, we adopt the methodology initially proposed by Colin de Verdière and Huck (1999) and later used by Arzel et al. (2006). This methodology is based on the analysis of both the spatio-temporal structure of the tracer anomalies (i.e temperature or salinity) controlling the circulation changes and the terms governing the density variance tendency in the North Atlantic sector. This approach led Arzel et al. (2006) to conclude that the nature of the instability driving the interdecadal oscillations under mixed boundary conditions is fundamentally different from that under flux boundary conditions.

Figure 11 shows that, by contrast to SSS anomalies, interdecadal North Atlantic [0–70°N] SST fluctuations in the present case appear to be nearly phase-locked to the strength of the AMOC. This relationship is an important
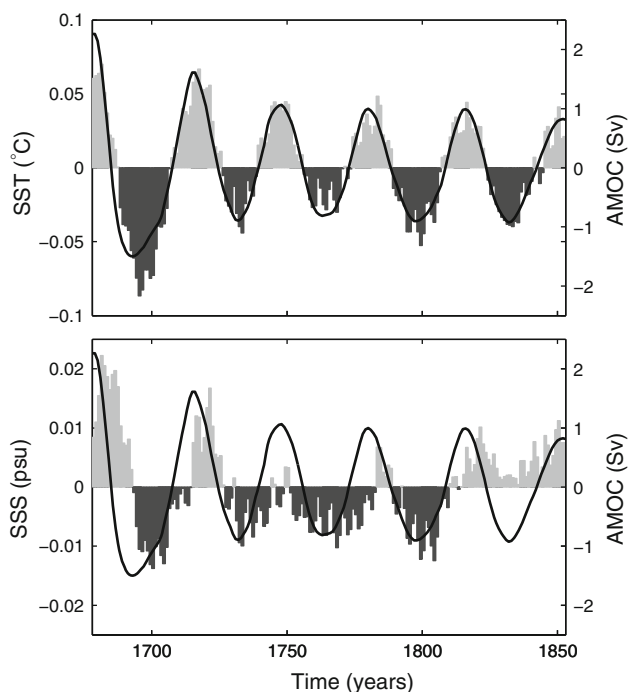
Fig. 11 Linearly detrended time series of maximum strength of the AMOC (*black solid line*), overlaid by detrended area weighted mean North Atlantic (0–70°N), **a** SST and **b** SSS annual mean anomalies during the first interstadial phase (years 1650–1850) of the glacial experiment using an atmospheric CO_2 concentration of 190 ppm and a freshwater forcing of −0.21 Sv (see Fig. 5). The AMO index corresponds to the SST timeseries in the *upper panel*

feature of interdecadal modes of variability simulated in a wide variety of ocean only and coupled climate models (Timmermann et al. 1998, among others; te Raa and Dijkstra 2002, among others; Knight et al. 2005, among others). Because this relationship suggests a dominant influence of temperature fluctuations on interdecadal timescales (∼30–40 years), the description that follows exclusively focuses on the origin and propagation of temperature rather than salinity anomalies.

Figure 12 shows the vertical structure of temperature anomalies in a quadrant taken from the western boundary

current region. Upper anomalies lag lower anomalies by about a quarter period. This peculiar phase shift is characteristic of the baroclinic instability mechanism which was shown to be at the heart of the existence of interdecadal modes of variability of the AMOC under steady surface buoyancy fluxes (Colin de Verdière and Huck 1999). This feature was also observed in a control simulation of the GFDL-CM2.1 model (Fig. 7 in Frankcombe et al. 2010) suggesting that the instability mechanism driving interdecadal climate fluctuations in this model is identical to the present one. A vertical phase shift is also apparent in the basin-averaged [85°W–5°E × 0–60°N] North Atlantic temperatures anomalies reconstructed from XBT data over the period 1960–1995 (Frankcombe et al. 2008). In order to get more confidence in the nature of the instability that operates on interdecadal time scales in the present model, it is instructive to compute the growth of temperature variance due to changes in surface heat flux, that is, the term $\overline{T'Q'}$ where the overbar denotes an average over several oscillation periods, and the prime the deviation therefrom. Figure 13 shows that the sign of $\overline{T'Q'}$ is negative everywhere and more particularly in the North Atlantic sector, demonstrating that changes in surface heat flux act to reduce SST variance. According to the study of Arzel et al. (2006), this demonstrates that the mechanism of interdecadal-interstadial variability in the UVic model is different from that operating under mixed boundary conditions where the growth of density variance was shown to be caused by the convective-surface heat flux feedback occurring in weakly stratified polar water columns. The 35 year variability is also characterized by a westward propagation of temperature anomalies (Fig. 14a), consistent with other climate models exhibiting variability on similar time scales (Arzel et al. 2007; te Raa and Dijkstra 2002; te Raa et al. 2004; Frankcombe et al. 2010). The amplitude of these anomalies is generally stronger at depth than in the mixed layer (not shown). This reduced surface signature is due to the damping by both infrared back radiation and turbulent air-sea heat fluxes. The spatial pattern of simulated SST

Fig. 12 Characteristic *z–t* diagram of the detrended temperature field horizontally averaged in the box area shown on the *left panel*, i.e (82.8–28.8°W × 30.6–41.4°N) computed over the first interstadial phase (years 1650–1850) of the glacial climate using an atmospheric CO_2 concentration of 190 ppm and an anomalous freshwater forcing of −0.21 Sv
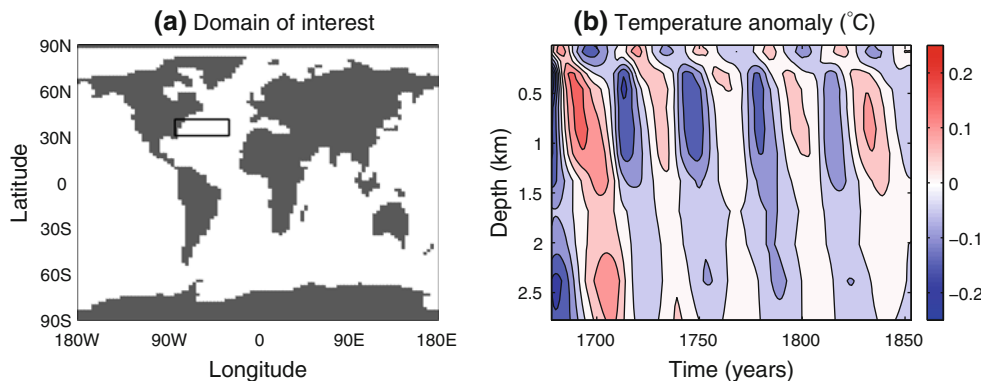
Fig. 13 Global distribution of the growth of temperature variance ($\overline{T'Q'}$, K^2 year^{-1}) due to surface heat flux (Q expressed in K year^{-1}) computed over the first interstadial phase (years 1650–1850) of the glacial climate using an atmospheric CO_2 concentrati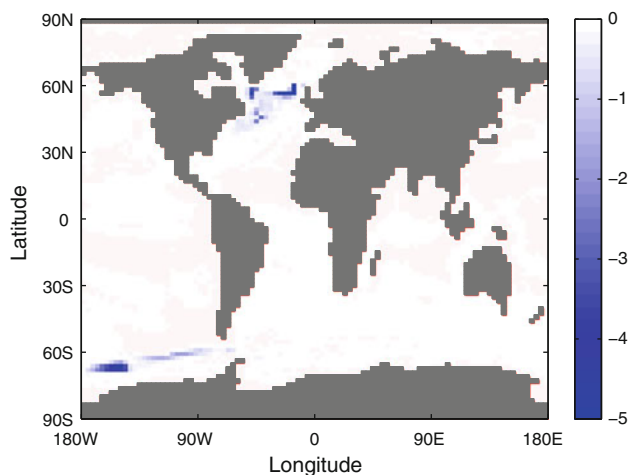on of 190 ppm and an anomalous freshwater forcing of -0.21 Sv. The overbar denotes an average over several oscillation periods, and the prime the deviation therefrom. The negative values indicate a damping of SST variance

gyre, and a cooling of smaller extent along the Gulf Stream path. The pattern is in good agreement with the same regression computed from raw annual data from 1955 to 2009 (Levitus et al. 2009). Applying time filtering and/or detrending does not significantly influence the North Atlantic pattern. The negative lobe in the western part of the domain around 40°N is not always apparent in AMO signatures, maybe because of the lower resolution of SST datasets on longer periods. The pattern shows some similarities with the SST differences between warm and cold periods on interdecadal time scales, as shown by Kushnir (1994) for instance. A similar pattern was also obtained in a control simulation of the GFDL-CM2.1 climate model (Msadek et al. 2010, auxiliary material Fig. S3b). The spatial extent of the surface signature simulated by UVic model is certainly smaller than that observed or that obtained in more realistic climate models (see Delworth et al. 2007). The reason is that the dynamical component of the atmosphere is prescribed in the UVic model. As such, atmospheric teleconnections and associated remote impacts due to changes in sea surface conditions of the North Atlantic area are much reduced in the UVic model. For instance, the climatic impact of the simulated interdecadal variability remains weak in the tropical Atlantic where changes in the strength of easterly trade winds and subsequent changes in latent heat fluxes are expected to affect the SST response when dynamical air-sea feedbacks are represented in a more realistic way.

Despite these differences and the different background climate employed here however, several fundamental features are in good agreement with modern observations (Frankcombe et al. 2008; Frankcombe and Dijkstra 2009) and other climate models (see references above), such as the vertical
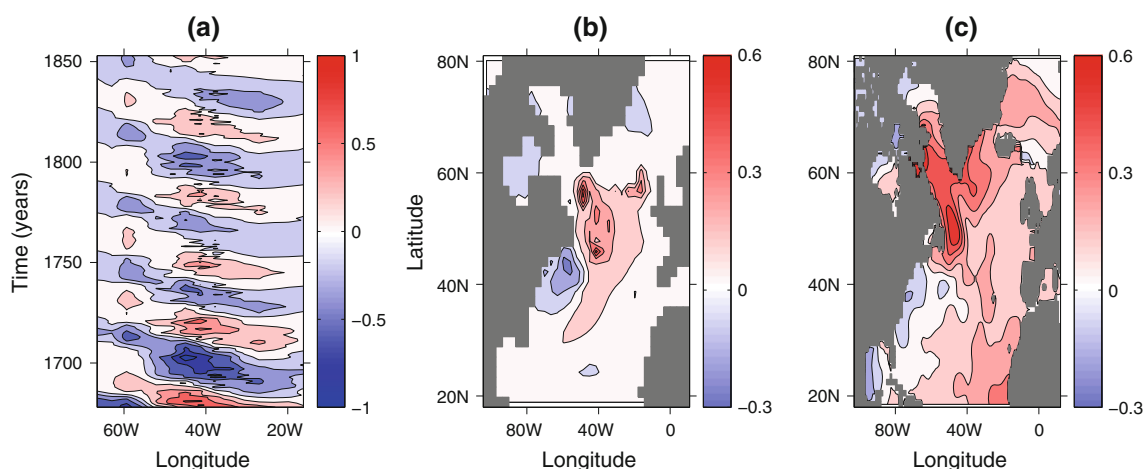
anomalies (Fig. 14b) is obtained through a regression of annual SST anomalies onto the AMO index, defined as the area-weighted mean timeseries of annual mean SST anomalies over the North Atlantic ocean (0–70°N). Since the AMO index is in phase with the strength of the AMOC (Fig. 11a), a very similar regression of SST anomalies onto the AMOC index results (not shown). The pattern reveals therefore that a strong AMOC is associated with a widespread warming extending from 30°N to 60°N in the North Atlantic sector, with maximum amplitude in the subpolar

Fig. 14 Surface temperature pattern associated with the first interstadial phase (years 1650–1850) of the glacial experiment using an atmospheric CO_2 concentration of 190 ppm and a freshwater forcing of -0.21 Sv. **a** Characteristic x–t diagram of meridionally averaged (43°N–54°N) SST anomalies in the Atlantic basin. **b, c** SST anomalies associated with one positive standard deviation of the AMO index, calculated by regression of surface temperatures with the index and multiplied by its standard deviation, similar to Knight et al. (2005), in the model (**b**) and in observations (**c**). See text for further details

structure and westward propagation of temperature anomalies in the extratropical North Atlantic. These similarities indicate the possibility of a physical mechanism similar to that driving the 30–40 years cycle associated with the AMO (Kerr 2000). The mechanism of which appears here to be identical to that obtained in stand-alone ocean models forced by fixed surface buoyancy fluxes, with the baroclinic instability mechanism being the trigger or wavemaker of interdecadal AMOC fluctuations during warm interstadials. Our conclusions therefore agree with those obtained by Arzel et al. (2010) who used a much simpler model.

Finally, it is natural to wonder why do interstadials give rise to interdecadal oscillations? The reason is that the growth rate of temperature anomalies (the salinity playing a secondary role, Arzel et al. 2006) associated with the baroclinic instability mechanism is intimately related to the strength of the AMOC, with increased growth rates associated with stronger circulations. This growth can however be limited by several processes, including horizontal mixing processes, air-sea turbulent heat fluxes and infrared back radiation as noted above. The efficiency of these sources and sinks of energy depend on the state of the system which, obviously, varies with time during the course of an oscillation cycle. Maximum growth rates are thus restricted to the warmest (transitory) phase of interstadials, where the AMOC is stronger, which may explain why interdecadal oscillations in Arzel et al. (2010) are restricted to that period. In the present case however, interdecadal oscillations can persist across whole interstadials, indicating that the energy source associated with the instability of the circulation is stronger than the sum of all energy sinks. Our simulations shows that this is most often the case, but not always. Because the net growth of temperature anomalies critically depends on the characteristics of the state of the coupled system, any differences between two interstadials can lead to very different signatures of interdecadal variability during those periods. The absence of such interdecadal cycles in the preindustrial and glacial experiments without DO type oscillations can then be attributed to a too weak AMOC.

8 Summary

On the basis of a large number of numerical experiments realized with the global coupled model of intermediate complexity UVic, we have analysed the bifurcation structure of the AMOC under different background climate conditions, under steady external (solar) forcing, prescribed ice-sheet topography, fixed seasonal cycle of surface wind stress, but in the absence of geostrophic turbulence in both the atmosphere and the ocean.

Abrupt millennial-scale climate transitions, whose general pattern qualitatively agrees with observed DO cycles, are shown to emerge spontaneously in a range of freshwater fluxes when the background climate is cold enough. In agreement with previous studies based on idealized climate models (Colin de Verdière and te Raa 2010; Arzel et al. 2010), the existence of such internal oscillations is shown to be caused by the relatively weak oceanic heat transport in the Atlantic basin. This is confirmed through a series of numerical experiments designed to explore the sensitivity of the bifurcation structure of the glacial AMOC to increased atmospheric CO_2 levels. Our results therefore strongly support the idea that DO events are the consequence of the weakening of the negative temperature-advection feedback. As the climate cools down, the stabilizing influence of this negative feedback on the circulation weakens. Millennial oscillations develop when the strength of this feedback and of the positive salt-advection feedback become comparable to each other. However, even for glacial climate conditions using prescribed ice-sheet topography at 19 ka, millennial oscillations are not guaranteed to emerge if the climate is too warm. This is due to an instability of the sea ice edge in response to increasing atmospheric CO_2 levels. Beyond a certain CO_2 threshold, Arctic sea ice coverage under glacial boundary conditions is found to be set up into a state similar to that obtained under preindustrial climate conditions. This significantly increases the temperature stratification at depths where the AMOC operates, thereby increasing the amount of heat carried from low to high latitudes, and ultimately stabilizing the circulation. In addition, the domain of existence of millennial oscillations is shown to be sensitive to the amount of CO_2 in the atmosphere. This occurs through a modification of sea ice properties (thickness and concentration) which affect the amount of freshwater delivery to NADW formation sites. In summary, these analyses highlight the important role of sea ice in controlling the behaviour of the coupled system on millennial time scales. Relatively small changes in both its concentration and thickness, without necessarily implying a change in its coverage, can significantly affect the domain of existence of millennial oscillations through of a modification of the surface freshwater budget at deep water formation sites. More substantial changes in its coverage can significantly affect the stability of the circulation through a modification of the temperature stratification and northward oceanic heat transport in the Atlantic basin. Last, but not least, our results support previous studies carried out with idealized climate models that the plateau phase during interstadials owes its existence to the influence of the ghost of the nearby saddle node (Colin de Verdière 2007; Arzel et al. 2010).

Another interesting feature of these millennial oscillations is the occurence of strong interdecadal oscillations of the AMOC during warm interstadials, while stadials

remains more stable with no oscillations at all. The mechanism of these interdecadal-interstadial oscillations is shown to be identical to that operating in ocean-only models forced by fixed surface buoyancy fluxes, in agreement with idealized studies carried out by Arzel et al. (2010). These oscillations were shown to develop when the strength of the AMOC is large enough (Huck et al. 1999), consistent with stronger interstadial circulations. The instability driving these interdecadal climate fluctuations was found to be a large-scale baroclinic instability in the vicinity of the western boundary current (Colin de Verdière and Huck 1999). The phase shift of a quarter period around the Gulf Stream path between upper and lower temperature anomalies, the westward propagation of subsurface temperature anomalies, and the phasing of North Atlantic SST anomalies with the AMOC index are all important features of these oscillations that are seen in the present study and were seen in a variety of coupled climate models (Arzel et al. 2007; te Raa and Dijkstra 2002; te Raa et al. 2004; Frankcombe et al. 2010; Msadek et al. 2010) and modern observations (Frankcombe et al. 2008; Frankcombe and Dijkstra 2009). This therefore strongly suggests that the physical mechanism of interdecadal-interstadial oscillations in the present study is identical to that driving the 30–40 years time scale associated with the Atlantic Multidecadal Oscillation (AMO, Kerr 2000).

9 Discussion

The proposed mechanism offers a plausible alternative to stochastic or coherence resonance hypotheses for which the existence and characteristics of millennial variability critically depends on noise level, generally added to the simulated or prescribed freshwater forcing (see Monahan et al. 2008, for a review). By contrast to Winton (1997) where millennial oscillations were shown to be caused by a convective instability, originating from the nonlinearity of the seawater equation of state, the present study points instead to an advective instability, similar to previous idealized studies using a linear seawater equation of state. Can the proposed mechanism, based on a weaker oceanic heat transport, account for the millennial variability that prevailed during MIS 5 ($\sim$73.5–123 ka)? This period was characterized by relatively high sea level and CO_2 concentrations compared to full glacial conditions. The nature of the variability during that period appears to be quite different from that developing during MIS 3, with Greenland interstadials exhibiting a multi-millennial cooling trend sometimes followed by the presence of rebound-type events (Capron et al. 2010). These events are associated with a relatively small, but abrupt, Greenlandic temperature increase compared to the DO events that punctuated

MIS 3. Capron et al. (2010) suggested that these rebound events are the consequence of orbitally forced cooling during extended interglacial-like periods. This could have resulted in progressively larger northern latitude sea ice extent and saltier surface waters, ultimately leading to a small resumption of the AMOC. These events are thus interpreted as a response of the AMOC to time-varying solar forcing, a mechanism which is absent here. We therefore suggest that the physical mechanism we proposed, based on a weaker northward oceanic heat transport in the Atlantic basin, may be more relevant to the glacial abrupt variability observed during MIS 3 rather than MIS 5. Nevertheless, further investigations with a global coupled model will be needed to assess the combined influence of ice-sheet size, orbital parameters and CO_2 levels on the domain of existence and characteristics of deep decoupling oscillations, such as described in the present study.

Despite the complexity of the present coupled model, a number of physical processes have not been included. Some of them might have played a crucial role in the development of abrupt warming events during the last ice age, such as ice-sheet-ocean feedbacks as proposed by Schmittner et al. (2002) and Timmermann et al. (2003). The advantages associated with this simplification of the present coupled system are therefore used at the expense of hypotheses that cannot be tested. These advantages are related to the ability to apply methods usually employed in dynamical system theory, such as the construction of bifurcation diagrams. This methodology has been proven extremely successful here in determining causal relationships and the origin of the glacial abrupt variability.

Although the general pattern of the simulated millennial temperature changes in both the ocean and the atmosphere is similar to that observed (i.e the sawtooth pattern and the vertical structure of temperature changes in the extratopical ocean during stadials), the amplitude of the abrupt warming events in the North Atlantic remains much weaker (1–2°C) than those inferred from Greenland ice cores. This could either be due to the absence of wind-stress feedbacks in the UVic model, which can affect both sea ice export and extent, or to a strong topographic control of deep convection. The first possibility will be examined in a forthcoming paper using an idealized geometrical set-up of the UVic model. The bifurcation sequence of the AMOC obtained here under glacial climate conditions (stable thermal state–oscillations–stable thermal state–stable haline state) markedly differs from that obtained previously with idealized single-basin models (stable thermal state–oscillations–stable haline state). Apart from the details of model physics, numerical schemes and parameterizations, the most striking difference between the present global model and the previous ones used in idealized studies lies in the model geometry. It seems therefore natural to assess the robustness of the bifurcation

sequence of the AMOC to the added presence of an idealized Pacific basin under glacial boundary conditions. This will require further analyses in a separate study. Despite these differences, it is important to note that the previous idealized studies have indicated causes for the origins of millennial oscillations which are robust.

In summary, our results strongly support the idea that observed DO events are the signature of internal oscillations of thermohaline origin. In this context, other factors, such as stochastic forcing associated with either atmospheric synoptic variability or oceanic geostrophic turbulence, interactive winds, time varying solar forcing, and ice-sheet-ocean feedbacks, are all processes that might not be essential to the development of such oscillations. Reduced northward oceanic heat transport in the Atlantic basin during glacial times seems to be the key to the existence of such instabilities.

References

Arzel O, Colin de Verdière A, England MH (2010) The role of oceanic heat transport and wind-stress forcing in abrupt millennial-scale climate transitions. J Clim 23:2233–2256

Arzel O, Colin de Verdière A, Huck T (2007) On the origin of interdecadal oscillations in a coupled ocean-atmosphere model. Tellus 59:367–383

Arzel O, Huck T, Colin de Verdière A (2006) The different nature of interdecadal variability of the thermohaline circulation under mixed and flux boundary conditions. J Phys Oceanogr 36:1703–1718

Bitz CM, Holland MM, Weaver AJ, Eby M (2001) Simulating the ice-thickness distribution in a coupled climate model. J Geophys Res 106:2441–2464

Bond G et al (1992) Evidence for massive discharges of icebergs into the North Atlantic ocean during the last glacial period. Nature 360:245–249

Bryan K, Lewis L (1979) A water mass model of the world ocean. J Geophys Res 84:2503–2517

Capron E et al (2010) Millennial and sub-millennial scale climatic variations recorded in polar ice cores over the last glacial period. Clim Past 6:345–365

Clement AC, Peterson LC (2008) Mechanisms of abrupt climate change of the last glacial period. Rev Geophys 46, doi:10.1029/2006RG000204

Colin de Verdière A (2007) A simple model of millennial oscillations of the thermohaline circulation. J Phys Oceanogr 37:1142–1155

Colin de Verdière A, Huck T (1999) Baroclinic instability: an oceanic wavemaker for interdecadal variability. J Phys Oceanogr 29:893–910

Colin de Verdière A, te Raa L (2010) Weak oceanic heat transport as a cause of the instability of glacial climates. Clim Dyn 35:1237–1256

Dansgaard W et al (1993) Evidence for general instability of past climate from a 250-kyr ice-core record. Nature 364:218–220

Delworth TL, Zhang R, Mann ME (2007) Decadal to centennial variability of the Atlantic from observations and models. Ocean circulation: mechanisms and impacts. Geophys Monogr 173:131–148

Eisenman I, Bitz CM, Tziperman E (2009) Rain driven by receding ice sheets as a cause of past climate change. Paleoceanograph 24, doi:10.1029/2009PA001778

Frankcombe LM, Dijkstra HA (2009) Coherent multidecadal variability in North Atlantic sea level. Geophys Res Lett, doi:10.029/2009GL039455

Frankcombe LM, Dijkstra HA, von der Heydt A (2008) Sub-surface signatures of the Atlantic Multidecadal Oscillation. Geophys Res Lett 35, doi:10.029/2008GL034989

Frankcombe LM, von der Heydt A, Dijkstra HA (2010) North Atlantic multidecadal climate variability: an investigation of dominant time scales and processes. J Clim 23:3626–3638

Gent PR, McWilliams JC (1990) Isopycnal mixing in ocean circulation models. J Phys Oceanogr 20:150–155

Greatbatch RJ, Zhang S (1995) An interdecadal oscillation in an idealized ocean basin forced by constant heat flux. J Clim 8:81–91

Griffies SM et al (2005) Formulation of an ocean model for global climate simulations. Ocean Sci 1:45–79

Huck T, Colin de Verdière A, Weaver A (1999) Interdecadal variability of the thermohaline circulation in box-ocean models forced by fixed surface fluxes. J Phys Oceanogr 29:865–892

Huck T, Vallis G, Colin de Verdière A (2001) On the robustness of the interdecadal modes of the thermohaline circulation. J Clim 14:940–963

Kageyama M, Paul A, Roche DM, Meerbeeck CJV (2010) Modelling glacial climatic millennial-scale variability related to changes in the Atlantic meridional overturning circulation: a review. Quat Sci Rev 29:2931–2956

Kalnay E et al (1996) The NCEP/NCAR 40 year reanalysis project. Bull Am Meteorol Soc 77:437–471

Kerr RA (2000) A North Atlantic climate pacemaker for the centuries. Science 288:1984–1986

Knight JR, Allan RJ, Folland CK, Vellinga M, Mann ME (2005) A signature of persistent natural thermohaline circulation cycles in observed climate. Geophys Res Lett 32, doi:10.1029/2005GL024233

Kucera M et al. (2005) Reconstruction of sea-surface temperatures from assemblages of planktonic foraminifera: multi-technique approach based on geographically constrained calibration data sets and its application to glacial Atlantic and Pacific Oceans. Quat Sci Rev 24:951–998

Kushnir Y (1994) Interdecadal variations in North Atlantic sea surface temperature and associated atmospheric conditions. J Clim 7:141–157

Levitus S, Antonov JI, Boyer TP, Locarnini RA, Garcia HE, Mishonov AV (2009) Global ocean heat content 1955–2008 in light of recently revealed instrumentation problems. Geophys Res Lett 36, doi:10.1029/2008GL037155

Levitus S, Boyer T (1994) World Ocean Atlas 1994. Volume 4: Temperature. NOAA Atlas NESDIS 3. U.S. Department of Commerce, Washington, DC

Levitus S, Burgett R, Boyer T (1994) World Ocean Atlas 1994. Volume 3: Salinity. NOAA Atlas NESDIS 3. U.S. Department of Commerce. Washington, DC

Li C, Battisti DS, Bitz CM (2010) Can North Atlantic sea ice anomalies account for Dansgaard-Oeschger climate signals? J Clim 23:5457–5475

Lopez-Martinez C, Grimalt JO, Hoogakker B, Gruetzner J, Vautravers MJ, McCave IN (2006) Abrupt wind regimes changes in the

North Atlantic ocean during the past 30,000–60,000 years. Paleoceanography 41, doi:10.1029/2006PA001275

Loulergue L et al. (2008) Orbital and millennial-scale features of atmospheric CH4 over the past 800,000 years. Nature 453: 383–386

Loving JL, Vallis GK (2005) Mechanisms for climate variability during glacial and interglacial periods. Paleoceanography 20, doi:10.1029/2004PA001113

Mann ME, Bradley RS, Hughes MK (1998 Global-scale temperature patterns and climate forcing over the past six centuries. Nature 392:779–787

Marotzke J (1996) In: Anderson, DLT, Willebrand J (ed) Analysis of thermohaline feedbacks, Series I Decadal climate variability: dynamics and predictability, vol 44. NATO ASI Series, pp 333–378

Masson-Delmotte V et al. (2005) GRIP deuterium excess reveals rapid and orbital-scale changes in Greenland moisture origin Science 309:118–121

Monahan AH, Alexander J, Weaver A (2008) Stochastic models of the meridional overturning circulation: time scales and patterns of variability. Philos Trans R Soc A 366:2527–2544

Msadek R, Dixon KW, Delworth TL, Hurlin (2010) Assessing the predictability of the Atlantic meridional overturning circulation and associated fingerprints. Geophys Res Lett 37, doi: 10.1029/2010GL044517

Pacanowski R (1996) MOM 2 documentation user's guide and reference manual. Version 2.0. Geophysical Fluid Dynamics Laboratory Ocean Technical Report. NOAA, GFDL

Paul A, Schulz M (2002) Holocene climate variability on centennial-to-millennial time scales: 2. internal feedbacks and external forcings as possible causes. In: Wefer G, Berger WH, Behre K-E, Jansen E (eds) Climate development and history of the North Atlantic Realm. Springer, Berlin, pp 55–73

Peltier WR (1994) Ice age paleotopography. Science 265:195–201

Rasmussen SO et al (2006) A new Greenland ice core chronology for the last glacial termination. J Geophys Res 111, doi:10.1029/2005JD006079

Rasmussen TL, Thomsen E (2004) The role of the North Atlantic Drift in the millennial timescale glacial climate fluctuations. Palaeogeogr Palaeoclimatol Palaeoecol 210:101–116

Rayner NA, Parker DE, Horton EB, Folland CK, Alexander LV, Rowell DP, Kent EC, Kaplan A (2003) Global analyses of sea surface temperature, sea ice, and night marine air temperature since the late nineteenth century. J Geophys Res 108, doi: 10.1029/2000JC000542

Roe GH, Lindzen RS (2001) The mutual interaction between continental-scale ice sheets and atmospheric stationary waves. J Clim 14:1450–1465

Sakai K, Peltier WR (1997) Dansgaard-Oeschger oscillations in a coupled atmosphere-ocean climate model. J Clim 10:949–970

Schmittner A, Yoshimori M, Weaver AJ (2002) Instability of glacial climate in a model of the ocean-atmosphere-cryosphere system. Science 295:1489–1493

Steffensen JP et al (2008) High-resolution Greenland ice core data show abrupt climate change happens in few years. Nature 321:680–684

Svensson A et al. (2008) A 60,000 year Greenland stratigraphic ice core chronology. Clim Past 4:47–57

te Raa LA, Dijkstra HA (2002) Instability of the thermohaline circulation on interdecadal timescales. J Phys Oceanogr 32:138–160

te Raa LA, Gerrits J, Dijkstra HA (2004) Identification of the mechanism of interdecadal variability in the north atlantic ocean. J Phys Oceanogr 34:2792–2807

Timmermann A, Gildor H, Schultz M, Tziperman E (2003) Coherent resonant millennial-scale climate oscillations triggered by massive meltwater pulses. J Clim 16:2569–2585

Timmermann A, Latif M, Voss R, Grtzner A (1998) Northern hemispheric interdecadal variability: a coupled air-sea mode. J Clim 11:1906–1931

Weaver AJ et al (2001) The UVic earth system climate model: model description, climatology, and applications to past, present and future climates. Atmos Ocean 34:1067–1109

Winton M (1997) The effect of cold climate upon North Atlantic Deep Water formation in a simple ocean-atmosphere model. J Clim 10:37–51

Winton M, Sarachik ES (1993) Thermohaline oscillations induced by strong steady salinity forcing of ocean general circulation models. J Phys Oceanogr 23:1389–1410

Wolff EW, Chappellaz J, Blunier T, Rasmussen SO, Svensson A (2010) Millennial-scale variability during the last glacial: the ice core record. Quat Sci Rev 29:2828–2838

Wunsch C(2006) Abrupt climate change: an alternative view. Quat Res 65:191–203

Yin J, Stouffer RJ, Spelman MJ, Griffies SM (2010) Evaluating the uncertainty induced by the virtual salt flux assumption in climate simulations and future projections. J Clim 23:80–96